rapporti

tecnici

Mounting calibration procedure to colorize point clouds of REIGL VZ-1000 using RiSCAN PRO® software

267

Istituto Nazionale di
Geofisica e Vulcanologia

rapporti tecnici

INGV

MOUNTING CALIBRATION PROCEDURE TO COLORIZE POINT CLOUDS OF REIGL VZ-1000 USING RISCAN PRO® SOFTWARE

Teresa Caputo[1], Renato Somma[1], Ermanno Marino[2], Claudia Troise[1], Giuseppe De Natale[1]

[1]**INGV** (Istituto Nazionale di Geofisica e Vulcanologia, Sezione di Napoli - Osservatorio Vesuviano)
[2]**STAGE s.r.l, Marcianise CE (Italy)**

267

Index

Introduction

In the framework of the national project MONICA (*MONitoraggio Innovativo per le Coste e l'Ambiente marino*) funded by the Italian Research Department, an innovative apparatus for coastal cliffs monitoring was acquired. The advanced monitoring system is ensured by a Terrestrial Laser Scanning (TLS). In particular it provides an useful support for the realization of the detailed 3D morphology reconstruction. This in turn is a very useful tool for the analysis of stability of coastal slopes affected by landslides in north-western sector of the Gulf of Pozzuoli. The instrument used is a long range TLS manufactured by RIEGL Ltd, model VZ 1000 ® equipped with a camera and a GPS positioned on top of it.

In recent years the TLS had a large range of applications in the studies concerning different environmental problems through the possibility of realizing high resolution Digital Surface Model (DSM) and Digital Terrain Model (DTM). Nowadays thanks to its aptitude, this instrument has been applied to monitoring occurrence of instability such as rock fall [Abellán et al., 2006, Abellán et al., 2013], landslides [Rowlands et al., 2003; Bitelli et al., 2004] and lava flow in volcano areas [Hunter et al., 2003] in order to quantify the natural hazards involved.

The TLS is a remote sensing technique used also as method for monitoring at fine scale the displacements. While the topographic monitoring method uses individual points for evaluating the displacements, the TLS produce a dense cloud of points. The multi-temporal comparison between calculated DTM obtained after the point clouds reconstruction can allows us to estimate the volumetric changes occurred. The TLS therefore produces a rich dataset which integrated with structural geology and geomorphological studies can allow us to understand the evolution of a defined area.

In this technical report we describe the procedure performed for the mounting calibration of the camera with respect to the laser scanner body. The aim is texturing adequately the point cloud with the pixels of the acquired RGB images contextually.

We describe the adopted calibration procedure. This latter turns out to be the first step for the future use of the instrument for the monitoring of the geomorphological modifications occurring along the cliffs of coastal areas belonging to the volcanic area with a high risk such as those of the Pozzuoli Gulf.

1. Laser scanner technology

The Light Amplification by Stimulated Emission of Radiation (LASER) was discovered by A. Einstein in 1917. He hypothesized that a ray of light of a certain frequency of incident an atom that emits a beam of high energy light that concentrates a great power in a very small area. Since 1999, the development and use of TLS. has seen a continuous expansion [Large and Heritage, 2009]. The main characteristics of these electromagnetic waves are summarized below:

- monochromatic (i.e. composed by a single light frequency);
- spatial coherence or unidirectional (i.e. the wave propagates at a great distance in a one direction);
- temporal coherence (i.e. waves of the same frequency and phase which are added together forming a wave high power train).

In other words, the laser radiation is a monochromatic light formed by parallel waves in phase between them.

The instrument is defined as an Electromagnetic Distance Meter (EDM). The distance measurement can be obtained through two types of approach: a) measure of the time of flight (TOF) and b) measure of the phase shift between the emitted wave and the received one. The first approach calculates the distances by time Δt employed by a transmitted pulse to return after it has been reflected. The propagation speed of the pulse is calculated by the traveled distance defined as:

$$[1] \qquad 2D = v \cdot \Delta t$$

The second process measures the phase difference between the emitted wave and the received one. In general, the distance is obtained as:

$$[2] \qquad D = \frac{\Delta \varphi}{2\pi} \frac{\lambda}{2} + n \frac{\lambda}{2}$$

Where $\Delta\varphi$ is the phase difference and λ is the wavelength.

The outcome of an acquisition will be a set of points in the space called cloud of points.

1.1 Technical data

The instrument here described is a long range laser scanner (TLS) based on the TOF manufactured by RIEGL, model VZ 1000 ® (http://www.riegl.com/) equipped with a 13 Megapixels external reflex digital camera (Nikon D90 ®) with a lens of 20 mm (Nikon AF 20 mm ®). The latter is mounted on the top of TLS. with a particular holder allowing to provide high resolution images. In this way it is possible to acquire in addition to the 3D point cloud also a RGB image of the area for making textures during post-processing.

The TLS. uses a narrow infrared (1550 nm) pulsed laser beam with pulse repetition rate (PRR) in the range from 70 to 300 kHz, so that in our case the 70 kHz can reaches 1400 m of distance. The minimum measurement distance is 2.5 m. The accuracy is 8 mm and the precision or degree to which further measurements show same results is 5 mm. In addition to the long range, a further advantage of this instrument is the data acquisition rate going from 29,000 point/seconds to 122,000 point/second at 70 and 300 kHz respectively. The horizontal scanning movement of the head rotating long Z-axis is very slow and is called *Frame Scan* with scan angle range from 0° up to max 360°. The movements long vertical line is very fast and it is due by rotating mirror and so called *Scan Line* with a scan angle range up to 100° (+130°/-30°). Both can be chose by the user. A clarification needs to be made on laser beam of the TLS and on its divergence. The laser beam is a cylindrical beam of photons that slightly deviates when it is emitted from the laser. When it moves away the beam begins to widen and at increasing in diameter. This is called the beam divergence.

The RIEGL VZ-1000 has a beam divergence of 0.3 mrad and an initial beam diameter of 7 mm. The spot size of the beam, at a given distance, can be calculated from the following equation [Pesci et al., 2011]:

$$[3] \qquad \theta = 2\arctan\left(\frac{D_f - D_i}{2l}\right)$$

Where θ is the beam divergence, D_f is the final beam diameter, D_i is the initial beam diameter and l is the distance traveled. This relationship is useful for calculating where to locate the instrument in accordance with the size of the target to detect. The typical beam divergence of the 0.3 mrad correspond to a 37 mm increase of beam width per 100 m of range.

The wavelength is near to infrared what makes it to belong to the class laser 1 (< 0,04 mW) therefore safe for user in according to the Standard EN60825-1:2007 on "Safety of the laser product - Part 1: equipment classification, requirements", equivalent to IEC 60825-1 ed2.0.

In particular the technology of this instrument is based on the number of measurements per laser pulse called multi-target 3D. Thanks to the online waveform processing this instrument is able to detect and process multiple echoes from the same direction. This means that it allows to discriminate each individual echo turning back along the same direction. It has a transmitter and receiver front end for each laser pulse. The laser beam is deflected fast rotating multi-facet polygonal mirror to acquire fast (see Figure 1). This mechanism is composing by a motorized three mirror faced symmetrically arranged around the rotation axis. When the laser pulse hits the edges of objects, a part of it came back and another part continues straight hitting objects placed at a greater distance. The pulse laser is reflected multiple times along the same direction resulting in more input echoes. This occurs especially when there is vegetation, fences and wires. The multi-target characteristic of the laser scanner allows to "cross" the tree leaves and then to "see" areas partially covered. The different incoming echoes are classified according to their progression in 'single', 'first', 'other' and 'last' target.

The data can be stored in different way. On internal flash memory card equipped inside the instrument up to 32 GByte, on external expandable memory card also up to 32 GByte or straight on a PC connect to the scanner via LAN, Wi-Fi or WLAN port. The scanner is provided of the internal GPS receiver (L1) for GPS time and global position. It can be changed with an external GPS receiver connected to the scanner. This is possible changing the GPS mode through the software. The external GPS provide an additional signal PPS (Pulse Per Second) that mark the change of a second. This latter is compared with scanner's internal time and the GPS time is inserted into the data stream.
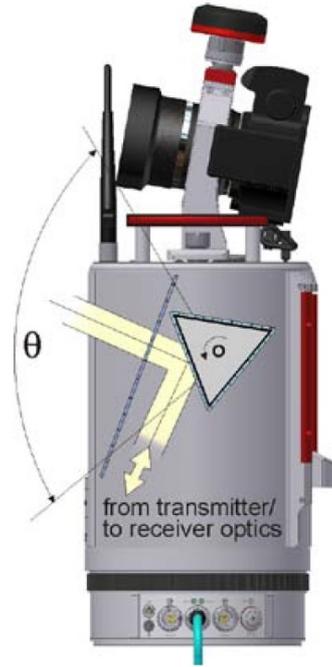
Figure 1. The laser beam transmitted/received and then deflected by a motorized three mirror.

1.2 Outcome of scanning

When a laser pulse hits a surface a part of the energy is absorbed, a portion is reflected and the other one is transmitted, according to the energy conservation principle expressed as:

$$[4] \qquad \alpha + \rho + \tau = 1$$

where α is the absorbed energy, ρ is the reflected energy and τ is the transmitted one. Each term is a dimensionless ratio with the incident energy.

The long-range TLS records the coordinates of ground points in 3D with an high velocity and accuracy in addition to the values as timestamp (that is a sequence of characters that identify an instant of time) amplitude, reflectance and pulse shape deviation. In the following the physical interpretation of the different outcome for each scanning will be describe.

The amplitude values provided by the instrument are calibrated. This latter is a signal property of the received optical target echo signal and is defined as the ratio of the actual detected optical amplitude versus the detection threshold. The amplitude value are scaled in dB. Also for the reflectance is a calibrated value. The reflectance of laser pulse depends on the roughness of the surface of the material hit. In particular, its behavior is governed by the Rayleigh criteria for which a surface is regarded rough when:

$$[5] \qquad \Delta h \geq \frac{\lambda}{8 \cdot \cos\theta}$$

where:

Δh is the vertical dimension of the average surface roughness of the surface (m), λ is the wavelength of the incident radiation (m) and θ is the angle of incidence of the wave respect to the vertical (rad).

The perfectly smooth surface reflected in a specular way, those rough instead behave as reflectors, then the direction of reflection is independent by the incidence one (see Figure 2). In real case the surfaces behave as intermediate cases. A special case are the retro-reflective surfaces. In this case the reflected beam propagates exactly along the same direction of the incident ray.
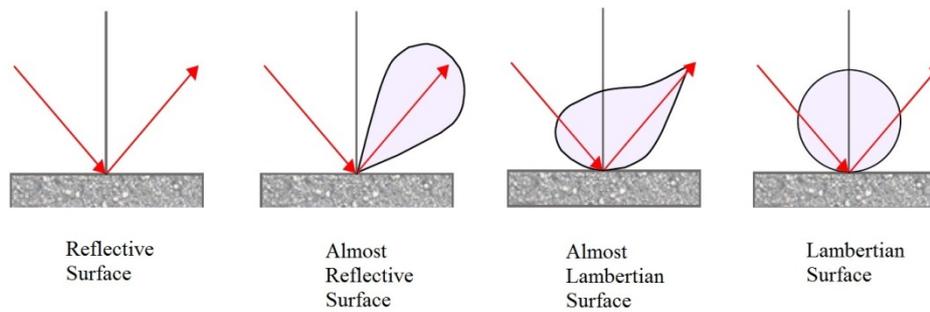
Figure 2. Behavior of surface at incident ray.

In this case the ratio of the target echo versus the calibrated amplitude value of a diffusely reflecting white target at the same distance. It is a dimensionless ratio empirical, its value range between 0 and 1 and its logarithm between -∞ and 0. The reflectance is a property that depended only by target surface reflectance respect to a white target.

The pulse shape deviation is still a ratio which describes the change of the received echo pulse shape compared to the emitted pulse shape. For ideal case the deviation value is 0. This can occur only when the received pulse fits 100% of the emitted pulse. But this condition is just an ideal case. Because the target surface shape such us texture and orientation respect to laser beam will change the pulse shape causing an increase on the deviation value. This occurs on edges or foliage of the trees.

Finally the timestamp is an information on the internal time with a resolution of 4 nanoseconds or on a GPS timestamp. Typical GPS receivers provide 1 timestamp value per second, coupled with a precise signal indicating the change of second (PPS pulse).

2. Coordinate systems

The point cloud acquired from laser contains also geometry information on coordinate systems. The scans are always performed from different points of view or positions. This ensures a good coverage of the area to investigate and avoid shaded areas. Each scan is characterized by its coordinate system. In particular that relative to the scanner is called "Scanner's Own Coordinate System" (SOCS); the coordinate system defined by the user is called "Project Coordinate System" (PRCS); the coordinate system into which the PRCS is incorporated is the "Global Coordinate System" (GLCS); finally the coordinate system of the camera mounted on the top of the scanner is the "Camera Coordinate System" (CMCS). In figure 3 is showed general schematic of the 4 coordinate systems and how they relate to one another. In the example four scan coordinates (SOCS1-4) are registered together to create the overall project coordinates (PRCS). Then the GPS data are applied to the point cloud and the GLCS is created so the point cloud is georeferenced.
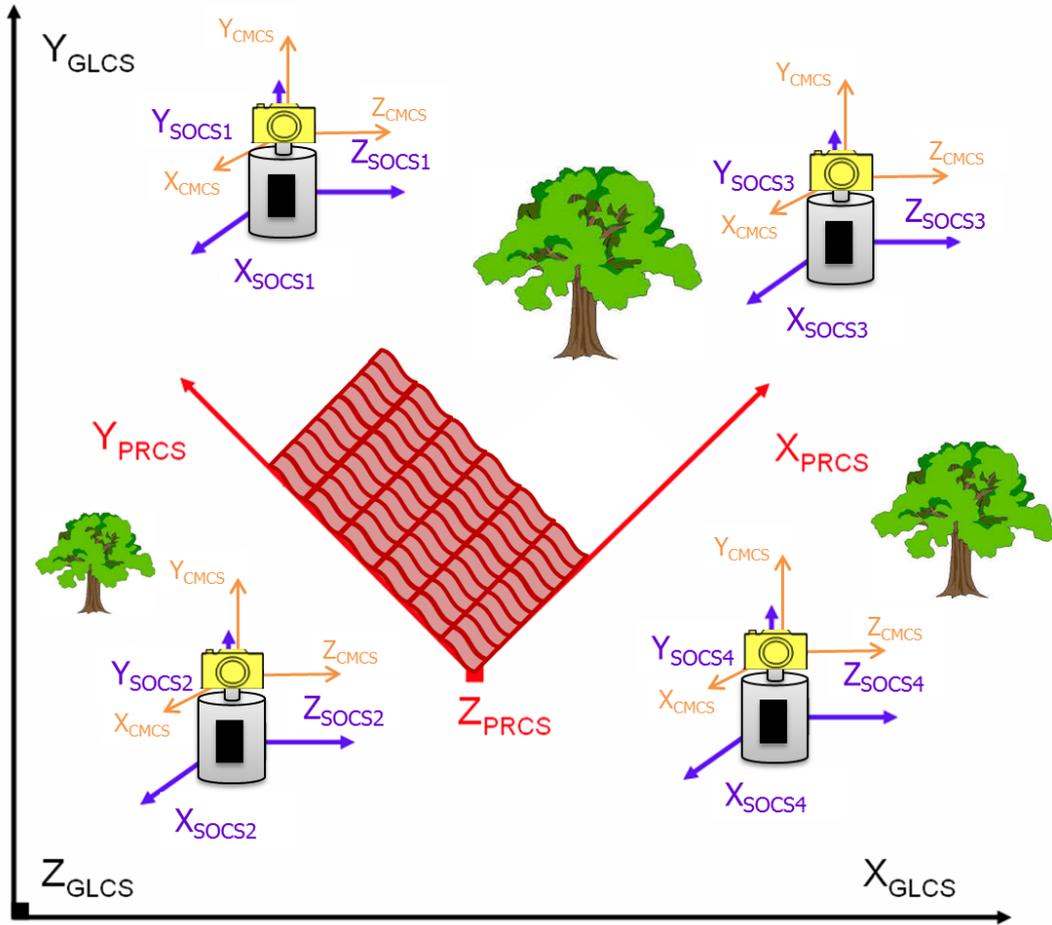
Figure 3. The general schematic of four coordinate systems (from http://www.unavco.org/ modified).

The software RiSCAN PRO®, (RiSCAN PRO Software Description & User's Instructions, 2013) to transform data from SOCS into the project coordinate system (PRCS) multiplies all its points with a matrix 4x4. This latter is defined "Sensor's Orientation and Position" matrix (MSOP). In case a data point P is need to be transformed from a specific scan position (point P_{SP^i}) into the GLCS, first multiply with the MSOP matrix of the scan position to get into the PRCS and subsequently multiply the point P_{PR}, with the "Project's Orientation and Position" matrix (MPOP) which transforms from the PRCS into the GLCS. Finally will be obtained the point P_{GL}, georeferenced. The followed sketch (Figure 4) show with an example this proceedings.
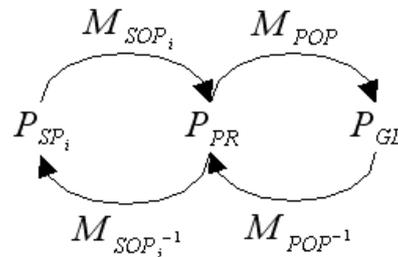
Figure 4. The sketch shows transformation from different coordinate systems SOC, PRCS, GLCS and vice versa.

The SOCS is different from the camera CMCS. Moreover, the direction of vectors of this latter follows the law of the right-handed, with x-axis upward, y-axis from left to right in the images and z-axis is the same of the center of view field of the camera (see Figure 5).

11
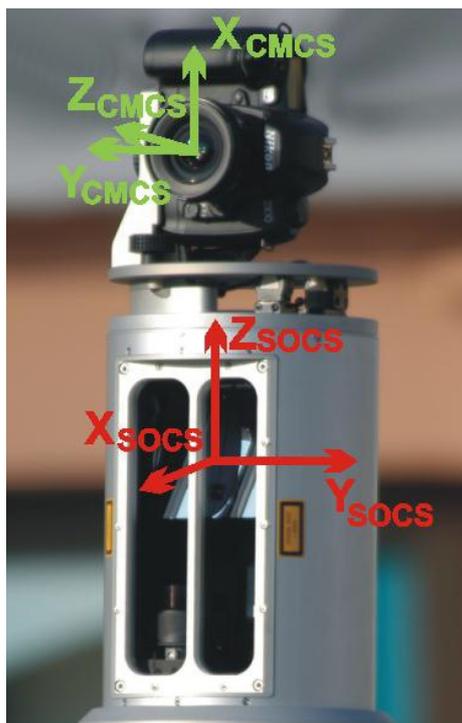
Figure 5. The different coordinate systems of the laser (SOCS) and camera (CMCS) respectively.

In order to texturized the cloud of points acquired in such a way that both the coordinate systems, SOCS and CMCS respectively, are coincident is necessary to apply a matrix consists of 9 parameters reflecting the rotation and 3 parameters relative to the translation. The purpose of this work is to show the procedure used for mounting device calibration of the camera. This procedure allows to find a matrix of rotation and translation between the pixels acquired from the camera and point clouds acquired from the scanner.

3. Software: RiSCAN PRO®

The point clouds obtained during a measurement are processed with specific software distributed by REIGL Ltd The software that allow the control of the instrument during the acquisition, the visualization and the processing is the RiSCAN PRO® (http://www.riegl.com/index.php?id=221). During the acquisition the data are organized and stored in a project structure. The data include scans, fine scans, digital images, GPS data, coordinates of points cloud and tie points, and all transformation matrices necessary to convert the data of multiple scans into a common well-defined coordinate system. In the figure 6 is shown the main program windows. It can be configured by the operator who can decide what tool windows should be displayed.

This software has several properties ranging from registration, filtering of data, triangulation, creation of orthophotos, computation of the volume of the objects represented by point clouds or meshes and finally animation of the shape of the object detected.

The process of registration of the various scans in the PRCS is the determination of the respective SOP (Sensor's Orientation and Position) matrix. The procedure for minimize the difference between points clouds is necessary to obtain one single point cloud and is done with three different methods as here described:

- through the local or global tie points coordinates;
- through an algorithm of the Iterative Closest Point (ICP) called multi station adjustment;
- through the procedure called back-sighting orientation with assigned coordinate known.

Filtering of data allow to manage the points cloud by defining filter operations, like the terrain filter can be used to separate off-terrain from terrain points.

The triangulation is the process of creating a surface out of a points cloud whereas the surface consists of triangles connecting the data points, also called "mesh". Furthermore the triangulated data can be textured with the high resolution images. The creation of orthophotos is performed with the aid of the acquired high resolution images.

The software carry the calibration parameters of camera and lens. This latter are interchangeable so it allows to choose the lens the suitable based on the image to be acquired.

This software also allows to perform the procedure mounting device calibration, which will be described in detail following.
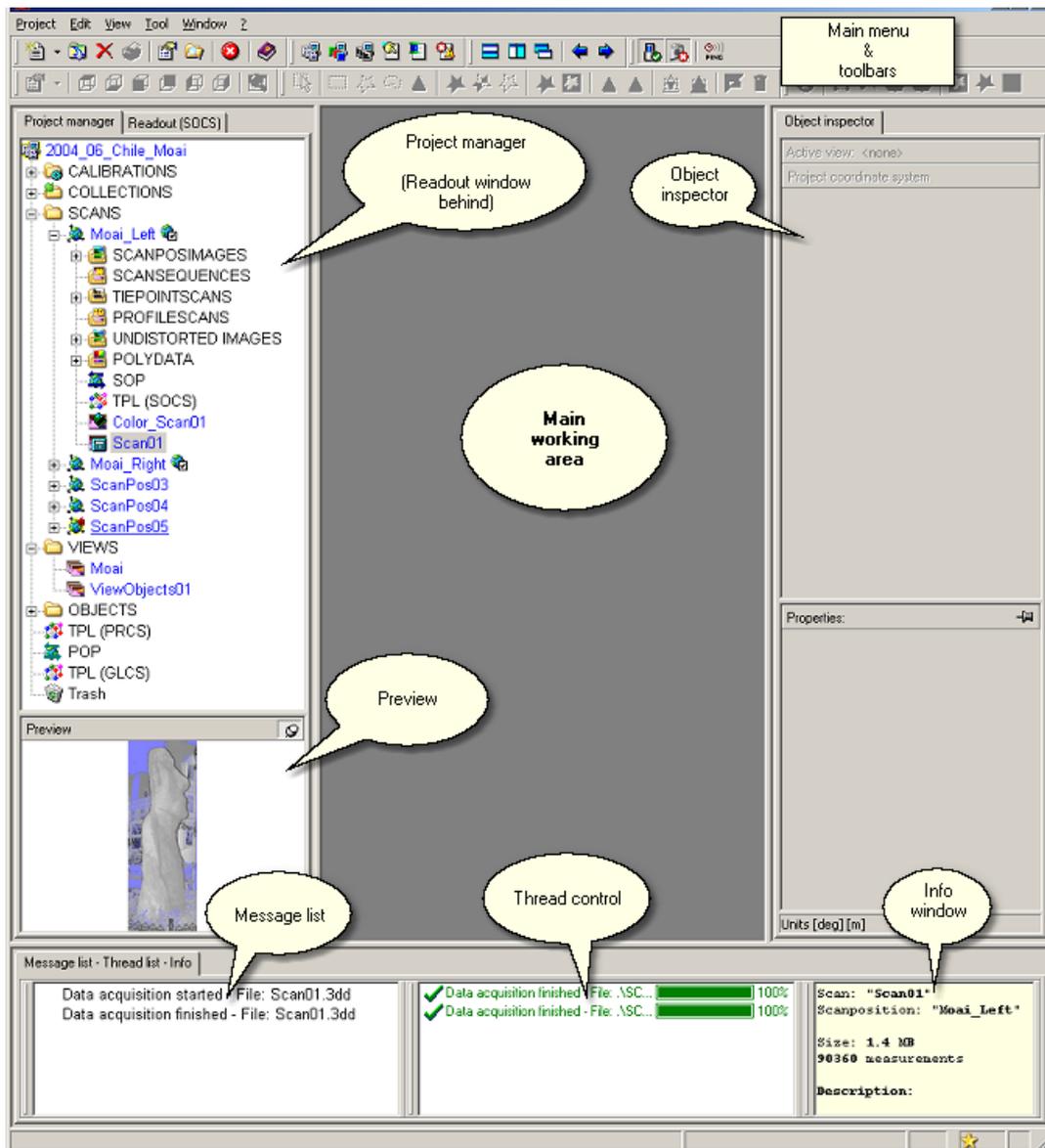
Figure 6. Tool windows of software RiSCAN PRO®.

4. Calibrations

In order to use the RGB images acquired simultaneously to the scans and then texture the points cloud, it is required to know the internal and external camera parameters. This allows to relate the camera field of view with the laser one.

The internal parameters depend on the type of camera and used lens. The external ones depend on relative positions between laser and camera when this last is mounted on top of the scanner. The software RiSCAN PRO® use a file called *camera calibration* file that define the internal and external calibration parameters (Figure 14). It contains information on the camera type, the lens type and mounting device. The laser scanner support different camera model. Also the lens are interchangeable to adapt them to different applications.

This file is composed by different information. The "general" is relative to camera information and its described is not used for any computation but as the internal calibration parameters are unique. It contains information on combination of the camera type and lens.

The "parameters" is relative to internal and intrinsic parameters of the camera. The intrinsic parameters dx and dy are the dimensions of a single pixel of the sensor. The Nx and Ny are simply the number of pixels in the horizontal direction and the vertical direction, respectively. This parameter is commonly specified by the manufacturer. The internal calibration parameters describing the focal length across two potentially different focal lengths (fx and fy). They are used to account for the potentially different pixel size in x and y direction and to account for different focal length of the lens (cylindrical lens error). The parameters fx and fy are normalized by the pixel size. The center of the image is (Cx, Cy) in pixels. Lens distortion is modeled by at least two radial and two tangential coefficients, k1, k2, p1, p2, respectively. The parameters k3 and k4 account for higher-order modeling of the radial distortion (RiSCAN PRO, 2013).

The external parameters related to the mounting device, "camera mounting", are given by geometry and orientation of the camera holder used (Figure 14). Its composed by 16 elements due to combinations of the translations and rotations matrix. All this parameters are necessary for the combination of the scans with images. This procedure is called texturing of point cloud. The pixel colors acquired by camera are extracted from the image and fused in the point cloud, so each point of the cloud is attributed the its correct color from the digital image [Abdelhafiz et al., 2005].

4.1 Camera Mounting Coordinate System (CMCS)

The camera is positioned on top of the instrument and aligned with the reference system of the scanner with a specific holder. Unlike the optical characteristics of the lenses, those of the mounting device are sensitive to the frequent use of the instrument. Simply mounting and disassemble the device from the top head of the instrument during the time can cause a going out of calibration . The first test that should be carried out as soon as the instrument is purchased is to verify the accuracy of the mounting calibration. Fast performing a scan of an area in order to verify the error texturing and therefore the need to calibrate the mounting and optionally also the parameters of the camera (lens).

Each calibration file describes the transformation associated with the mounting of the camera (CMCS) with respect to the scanners coordinate system (SOCS). The transformation is described by a rotation matrix R and a translation vector T.

$$[6] \qquad R = \begin{pmatrix} r_{11} & r_{12} & r_{13} \\ r_{21} & r_{22} & r_{23} \\ r_{31} & r_{32} & r_{33} \end{pmatrix} T = \begin{pmatrix} t_1 \\ t_2 \\ t_3 \end{pmatrix}$$

The camera on top of the instrument is mounted into the +x-direction of the SOCS system and is usually tilted by 90° around the camera's z-axis (Figure 2.). The standard rotation matrix is R_0 and the translation in the camera's coordinate system is 0.25 m above the origin of the scanner and 0.1 m in the direction of the camera's z-axis.

$$[7] \qquad R_0 = \begin{pmatrix} 0 & 0 & 1 \\ 0 & -1 & 0 \\ 1 & 0 & 0 \end{pmatrix} T_0 = \begin{pmatrix} -0.25 \\ 0.00 \\ -0.10 \end{pmatrix}$$

For convenience R and T are combined together to form a 4 x 4 matrix as the following equation:

$$[8] \qquad RT = \begin{pmatrix} r_{11} & r_{12} & r_{13} & t_1 \\ r_{21} & r_{22} & r_{23} & t_2 \\ r_{31} & r_{32} & r_{33} & t_3 \\ 0 & 0 & 0 & 1 \end{pmatrix}$$

These are default values provided by the manufacturer. Following will be described a procedure necessary to refine these distances and rotational and translation matrix.

4.2 Mounting calibration procedure

The original calibration file contains a series of information relative to the camera, the intrinsic and extrinsic parameters of the lens adopted, both belonging to the mounting parameters and the scanner. The lens of parameters are specified by the manufacturer and not require a correction because depending by camera model.

The mounting parameters are represented by a matrix that transforms the coordinates from SOCS in to CMCS system. The calibration is performed mounting the camera on the top of the scanner and the test, therefore is performed by the laser scanner in automatic mode in order to detect the targets. Typically, in a real test, a representative number of retro reflective targets are positioned along a vertical alignment in a scene in order to be identified by the camera. After this array has been positioned a series of images are acquired with using the flash in case of scarce light conditions, in this way the retro-reflectors positions are acquired. These latter are called tie-points and are clearly as amplitude data. The tie-point itself commonly represents the center of a reflective target. These objects can be easily found into the images acquired by the camera. In every image the centers of the reflectors are automatically extracted and are automatically linked to the 3D coordinates of the target. For this kind of test a total station is not required. In this way the quality of the mounting parameters are improved. During the mounting calibration the first step is to perform a 360° scan. In figure 7 is shown an detail of this overview which contain all reflectors positioned in the scene. The dimension of the targets used are the 0.10 m in diameter and flat shape. The software allow to choose to different reflectors in use during the data acquisition defining a reflector calibration from a list of the supported reflectors type such us sphere, cylinder, disc (flat), identifying also the color, diameter and height.

Figure 7. Scanning detail of overview with the identification of tiepoints.

The test was carry out in a closed environment (into the basement of the our building) with a good perspective depth. The second step is to extract the reflectors from the scan carry out, by the function "Find reflectors". This function extracts all retro-reflective objects from a scan and writes their coordinates into the corresponding tie-point list. Subsequently has been make a fine scan of all extracted reflectors, called tie-point scans (see Figure 8).
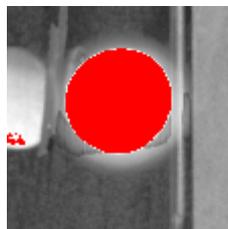
Figure 8. Fines can of target.

The next step is acquire an image containing all the positioned reflectors. In figure 9 is show the picture taken with flash mode and the reflectors positioned at different depth and height. The flash mode can be help to extract the reflectors in the image.

Figure 9. Image acquisition of target with dimension of 0,10 m. diameter.

For assisted calibration has been used a computer on which has been installed the RiSCAN PRO software ®. In order to manage the quality of the mounting adjustment is necessary to create a new mounting calibration. The software allow to improve the mounting calibration by importing already existing mounting calibration file from another project (see Figure 10).
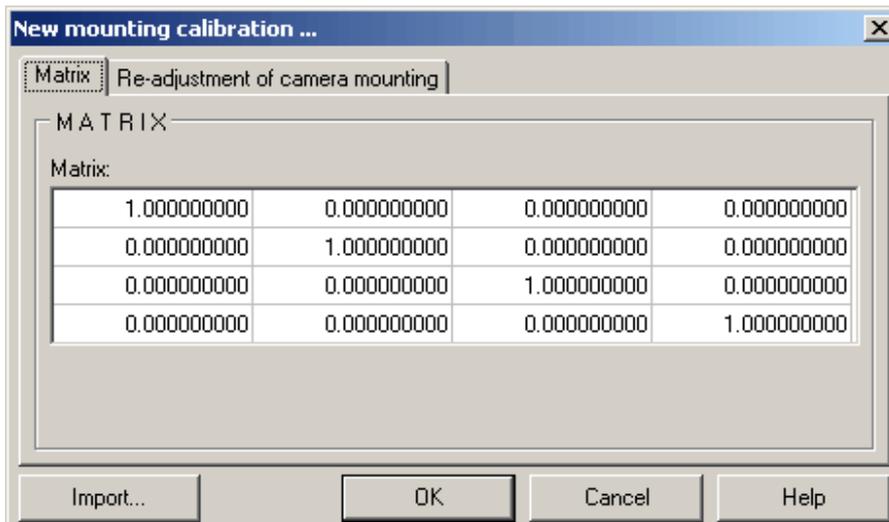
Figure 10. Screen shot of new mounting calibration function.

The extraction of the reflectors from scan and image respectively allow to link both pairs. The figure 11 shows a zoom on the image where has been active the display of the tie-point image (Image_tp0*) and tie-point (tp0*). The different position is given by a not perfectly calibrated mounting matrix.

Figure 11. Overlap by TPL(Tie Point List) image (Img_tp0*) and TPL (tp0*).

To improve the alignment has been find about ten correspondent pairs. Then the software allows to optimize the alignment through the function "Re-Adjustment of camera mounting" and searches all scan position for link established with the "Start re-adjustment" (see Figure 12). For optimization has been settings as well as calculation mode the modify rotation only. This latter optimizes only the three rotation parameters out of the six parameters defining the mounting calibration. Because the position of the camera is very well defined as well as is provided by the constructor. The figure of merit used has been the least squares fitting. The algorithm is based on minimizing the sum of the squares of the residuals. The drawback to this algorithm is that the result may be changed significantly even by a single outlier resulting from a wrong link. Therefore, is necessary to carefully check the link.

In the figure 12 is shown the results of the computations and in bottom, in the log area, is shown the improvement in the residual error between pixel distance, current and new.
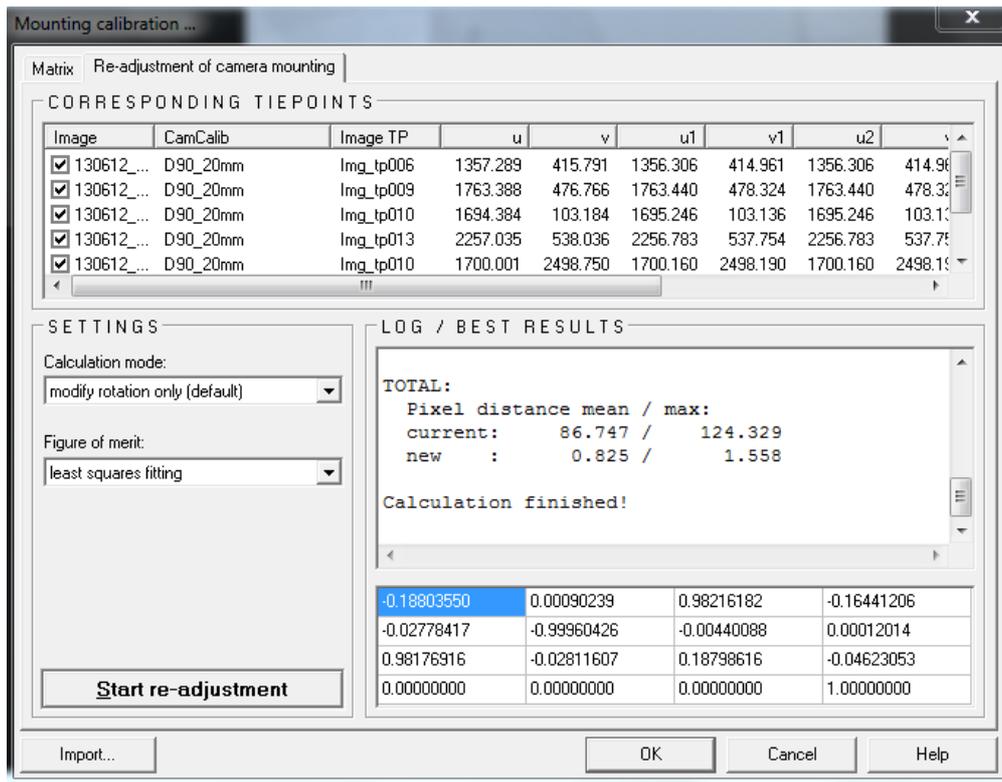
Figure 12. Start re-adjustment and log area with the improvement in the residual.

Finally a check of the quality is given by displaying the tie-points again within the image as shown in figure 13.

Figure 13. Overlap by TPL image (Imag_tp0*) and TPL (tp0*) after calibration procedure.

19

Successively is necessary to export the mounting calibration parameters calculated (see Figure 14) then to import from pc on project the file created as camera calibration that will be used by assign to image (see Figure 15). In figure 16 are shown the calculated parameters that compose it, as the type of camera, the internal parameters, those relating to the mounting device and the scanner itself.
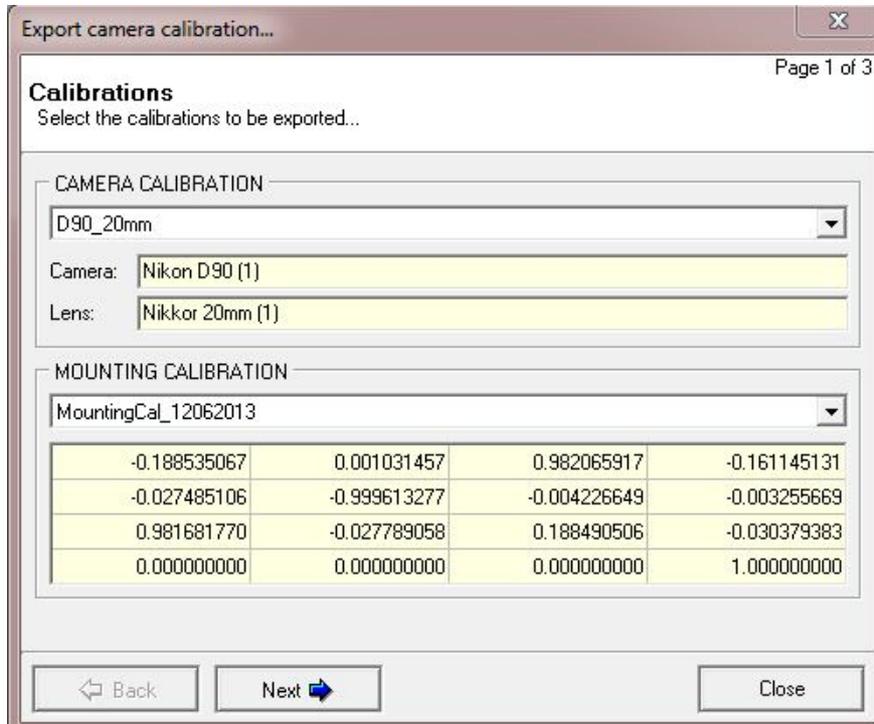
Figure 14. Screen shot showing function "Export camera calibration" where the mounting calibration parameter is calculated to be exported.
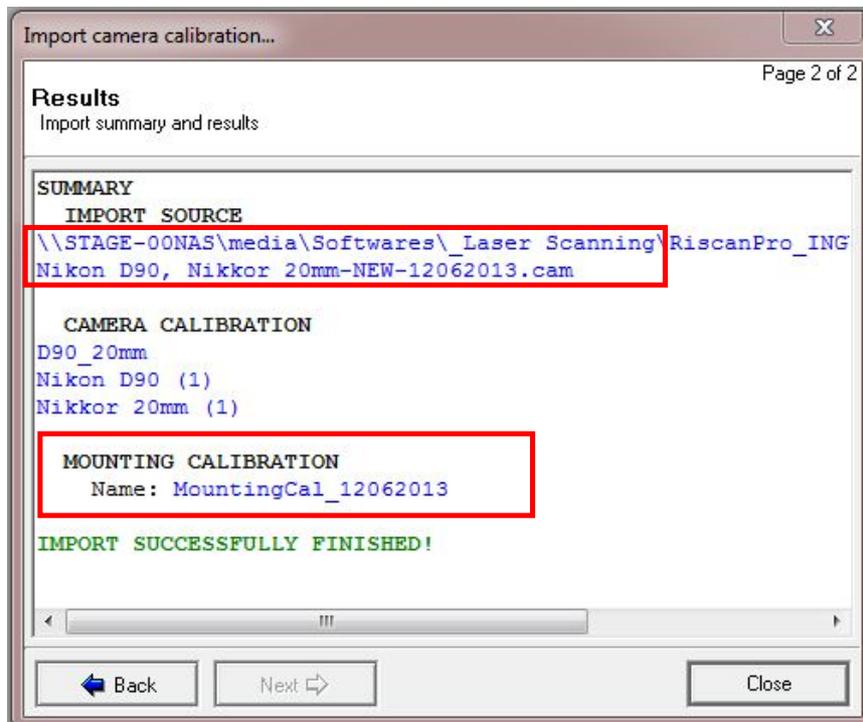
Figure 15. Screen shot showing the function "Import camera calibration" where is possible to import the file camera calibration created.

Figure 16. The contents of calibration file with different parts that composing it. In red box there is highlight the camera mounting parameters.

5. Result and conclusions

The success of the mounting calibration was subsequently tested in both indoor and outdoor conditions. The verification of indoor conditions the matrix of rotation and translation is efficient as shown by the overlapping between the two images A and B in figure 17. In image A was used the mounting calibration file by default. While in image B was used the new calibrated file. In image A is clearly visible an error in the texturization between the points cloud and the pixels of the photo, while in image B the overlapping in improved greatly.

Following an outdoor test was performed to check any problems of the texturization with major distances. In figure 18 was once again used the calibration file of default highlighting further that the gap increases with the distance. This is even more evident along the edges of the building. At a distance of 150 m there is a gap of about 5-6 m. Instead using the calibration file recalculated (see Figure 19) emerges clearly that the texturization shows a good match. The overlap between the points cloud around the windows, grid, and the edges of the building is good. As can be seen from the comparison between the figure 19 and the picture of the figure 20.

21
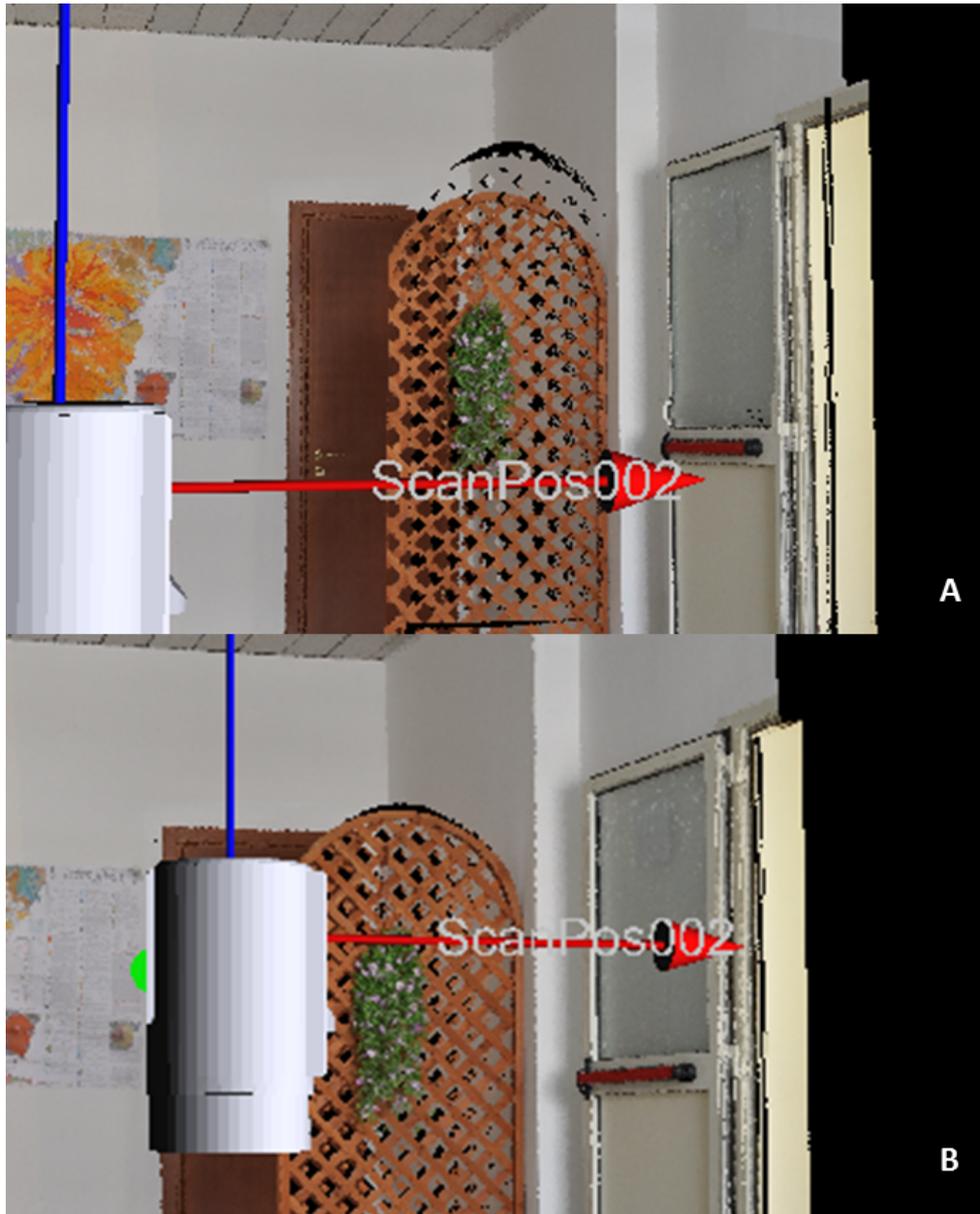
Figure 17. Comparison between two scans in indoor tests with and without the correction of the mounting of the camera. A) before correction. B) after correction.
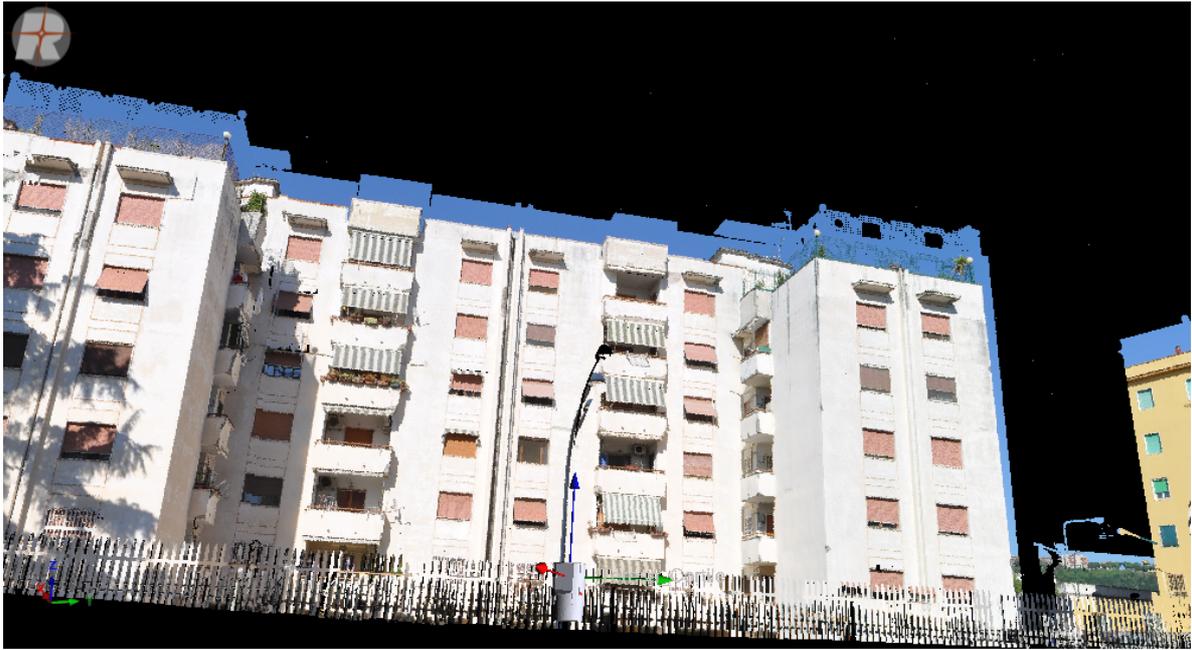
Figure 18. Scanning with texturing of the points cloud with incorrect mounting calibration files. See text for details.

Figure 19. Scanning with texturing of the points cloud with correct mounting calibration files.

Figure 20. Photo of the outdoor scene which was chosen.

Acknowledgments

References

Abdelhafiz A., Riedel B., Niemeier W., (2005). *Towards a 3D true colored space by the fusion of laser scanner point cloud and digital photos*. ISPRS Archives Volume XXXVI-5/W17, 2005 WG V/4 3D-ARCH 2005: Virtual Reconstruction and Visualization of Complex Architectures 22-24 August, 2005Mestre-Venice, Italy, Editor(s): Sabry El-Hakim, Fabio Remondino, Lorenzo Gonzo. Conference Paper.

Abellán A., Oppikofer T., Jaboyedoff M., Rosser Nicholas J., Lim M., and Lato Matthew J., (2013) *Terrestrial laser scanning of rock slope instabilities* Earth Surface Processes and Landforms, Volume 39, Issue 1, pages 80–97, January 2014 DOI: 10.1002/esp.3493

Abellán A., Vilaplana J.M., and Martinez J., (2006). *Application of a long-range terrestrial laser scanner to a detailed rockfall study at Vall de Nuria (Eastern Pyrenees, Spain)*. Eng Geol 88:136–148. doi: 10.1016/j.enggeo.2006.09.012.

IEC 60825-1 ed2.0 (2007). Safety of laser products - Part 1: Equipment classification and requirements (2007-03-30).

Hunter G., Pinkerton, H., Airey, R. and Calvari, S., (2003). *The application of a long-range laser scanner for monitoring volcanic activity on Mount Etna*. Journal of Volcanology and Geothermal Research 123, 203–210.

Pesci A., Teza G. and Bonali E., (2011) *Terrestrial Laser Scanner Resolution: Numerical Simulations and Experiments on Spatial Sampling Optimization*- Remote Sens. 2011, 3, 167-184; doi:10.3390/rs3010167.

Riegl, (2013). *Terrestrial Scanning*, http://www.riegl.com/nc/products/terrestrial-scanning/, Riegl Laser Measurement Systems GmbH, Horn, Austria

RiSCAN PRO, Software Description & User's Instructions, Version 1.7.8, June 2013.

Rowlands K.A., Jones L.D. and Whitworth M., (2003). *Landslide laser scanning: a new look at an old problem*. Quarterly Journal of Engineering Geology and Hydrogeology 36 (2), 155–157.

Bitelli G., Dubbini M. and Zanutta A., (2004). *Terrestrial Laser Scanning And Digital Photogrammetry Techniques To Monitor Landslide Bodies*. Proceedings of the XXth ISPRS congress, Istanbul, Turkey. Commission V, WG V/2.

Large A.R.G and Heritage G.L., (2009). *Laser Scanning – Evolution of the Discipline*. In: Laser Scanning for the Environmental Sciences (George L. Heritage and Andrew R.G. Large Eds.), pp. 1-20. Blackwell Publishing Ltd. ISBN: 978-1-405-15717-9.

http://www.ingv.it

Istituto Nazionale di Geofisica e Vulcanologia